Available online at BCREC website: https://bcrec.id

Bulletin of Chemical Reaction Engineering & Catalysis, 18 (3) 2023, 407-419

Research Article

Xylene Isomerization using Hierarchically Mesoporous ZSM-5

Ahmed El Fadaly[1], M.A. Sayed[1], Ahmed O. Abo El Naga[1,*], Mohamed El Saied[1], Seham A. Shaban[1], F.I. Elhosiny[2]

[1]Refining Division, Egyptian Petroleum Research Institute, 11727 Nasr City, Cairo, Egypt.
[2]Chemistry Department, Faculty of Science, Ain Shams University, Cairo, Egypt.

Received: 9th July 2023; Revised: 29th August 2023; Accepted: 30th August 2023
Available online: 7th September 2023; Published regularly: October 2023

Abstract

The current study described the synthesis of H-ZSM-5 zeolites with hierarchical micro-meso- porosity (HM-ZSM-5-x) via the soft-templating route, employing organosilane surfactant, 3-[(trimethoxysilyl) propyl]octyldimethyl-ammonium chloride, as the mesoporous template. The catalytic performance was examined in the isomerization of *o*-xylene in a fixed-bed reactor at atmospheric pressure. Many techniques were conducted to characterize the catalysts. The X-ray diffraction (XRD) and Fourier Transform Infra Red (FTIR) results affirmed that all mesoporous zeolites possess the characteristic MFI structure, as well as good crystallinity. The N_2 physisorption measurements signified that all HM-ZSM-5-x samples have higher surface areas and pore volumes than the micro-ZSM-5 sample, with the mesopores accounting for the vast majority of the total surface areas and pore volumes of HM-ZSM-5-x samples. Moreover, the mesoporosity of the obtained HM-ZSM-5-x zeolites can be simply tuned via the variation of the amount of TPOAC used. Compared with classical micro-ZSM-5, the HM-ZSM-5-0.15 sample possessed a higher *o*-xylene conversion and p-xylene yield that was attributed to its remarkable textural characteristics in terms of higher surface area and prevailing mesoporous character that led to a reduced diffusion limitation. Importantly, the catalyst manifested superb operational stability within 50 h, indicating high resistance against deactivation through coke deposition.

Keywords: Xylene isomerization; Hierarchical mesporosity; ZSM-5; Mesoporous ZSM-5; amphiphilic organosilane; soft template

How to Cite: A. El Fadaly, M. A. Sayed, A. O. Abo El Naga, M. El Saied, S. A. Shaban, F. I. Elhosiny (2023). Xylene Isomerization using Hierarchically Mesoporous ZSM-5. *Bulletin of Chemical Reaction Engineering & Catalysis*, 18(3), 407-419 (doi: 10.9767/bcrec.19270)

Permalink/DOI: https://doi.org/10.9767/bcrec.19270

1. Introduction

The three isomers of xylene, *ortho*-xylene (1,2-dimethyl benzene, ox), meta-xylene (1,3-dimethyl benzene, mx), and *para*-xylene (1,4-dimethyl benzene, px), are potential starting materials in the petrochemical industry since they are used for the production of a wide variety of industrially important products. These compounds are produced mostly from reformate, pyrolysis gasoline (pygas), and coke-oven [1–3]. o-xylene is used for manufacturing phthalic anhydride, which is used widely as a plasticizer. *m-xylene* is converted into isophthalic acid, a raw material for the production of unsaturated polyester resins, while *p-Xylene*, is oxidized to terephthalic acid, which is used in producing polyethylene terephthalate (PET) [1–3]. Among the three xylene isomers, *p-xylene* is the most demanded in the market, accounting for approximately 83 percent of the worldwide demand for

* Corresponding Author.
Email: : amo_epri@yahoo.com (A.O.A. El Naga);
Telp: +2-01874558262

xylenes [1,4–6]. The world demand for p-xylene has enormously increased over the past few years and is expected to increase in the future further [7]. Accordingly, isomerization of the low-valued of o- and m- xylene to p-xylene has attracted a great deal of attention in recent years [7].

Conventional HZSM-5 has been deemed an exceptional catalyst for xylene isomerization because of its high surface area, high (hydro)thermal stability, high acidity, and shape selectivity [6,7,8]. Though the microporous structure endows the zeolitic catalysts with properties that are highly advantageous to catalytic applications, it induces severe mass transport limitations, prohibiting the bulky reactant molecules from diffusion into the internal voids of zeolite to access the active sites, thus lowering the overall catalytic activity [9–13]. Additionally, the pure microporosity in zeolites may also make them more prone to rapid deactivation during catalysis arising from coke deposition [13–15].

An efficacious tactic to address the issues associated with zeolite microporosity is to incorporate a secondary mesoporous system inside the microporous zeolite framework, the so-called hierarchical meso-microporous zeolite [9,10,12,13,16,17]. The resultant hierarchical mesoporous catalyst will not only have an improved diffusion of the bulky m- and o-xylene to the catalytically active sites, and hence higher isomerization activity, but also maintain the shape selectivity of the microporous catalyst, which is responsible for high p-xylene selectivity. Moreover, the hierarchical zeolites present higher resistance to coke deposition [13,18]. For example, in 2010, Fernandez and co-workers [19] synthesized ZSM-5 zeolite with a hierarchical micro-mesoporous structure and scrutinized its catalytic performance for the shape-selective isomerization of o-xylene. The hierarchical ZSM-5 catalyst, which was obtained by post-synthesis desilication with NaOH followed by mild HCl washing, exhibited an approximately twofold increase in p-xylene yield compared to the conventional microporous counterpart. In a recent study by Zhou *et al*. [20], hierarchical mesoporous ZSM-5 zeolite was synthesized by steam-assisted crystallization and used for the o-xylene isomerization. The mesoporous ZSM-5 catalyst revealed a higher conversion of *o*-xylene than the conventional microporous catalyst due to the reduced diffusion limitation. However, the hierarchical ZSM-5 zeolite possessed a decreased selectivity to *p*-xylene in the products due to the lower shape selectivity of external acid sites.

Over the past few years, several strategies for the preparation of hierarchical mesostructured zeolites have been reported. Generally, these methods can be categorized into three classes, namely, assembly, demetallization, and mixed methods. Among these strategies, the assembly approach has enticed notable attention. The assembly methods involve the usage of mesopore templates to introduce the desired mesoporosity into zeolite crystals, in addition to the conventional zeolite structure directing agents responsible for micropore generation [14]. The assembly methods can further be sub-categorized into two types based on the physical state of the mesopore forming agent, viz., hard templating when the mesopore creator is insoluble in the synthesis gel and soft templating with soluble ones [10]. The hard or soft mesopore creators are incorporated into zeolite crystals during crystallization and then removed by means of combustion or acid dissolution leading to the formation of a hierarchical mesoporous zeolite. Compared to the hard template method, the soft-template one is simpler, faster, and relatively cost-effective [10].

In the soft templating approach, flexible species, such as surfactants and polymers, are used as mesopore-directing agents [10,16,21,22]. Materials need to satisfy the following prerequisites to be used as soft templates to synthesize hierarchical mesoporous zeolites [23]: (1) be chemically stable under the strong basic hydrothermal conditions in which zeolites are prepared, (2) be able to effectively interact with the silica species, (3) be cheap in order to make the large-scale production of mesoporous zeolites economically viable, and (4) have fiber-like morphology in aqueous solution. Throughout the last few years, several materials have been used as soft templates to synthesize hierarchical mesoporous zeolites [24–28]. Nevertheless, it was found that, in most cases, during the soft templating synthesis, the conventional structure directing agent and the soft mesopore creators operate competitively, leading to the formation of a separated mixture consisting of amorphous mesoporous siliceous material and crystalline zeolite with no mesoporosity [13,29].

To solve this situation, in 2006, Ryoo and co-workers [30], in their seminal work, proposed the usage of rationally designed amphiphilic organosilane surfactants as novel soft mesopore-forming agents. Templates of this class are constructed from three main components [14,31,32]: (1) hydrolysable alkoxysilane moiety that can effectively interact with the SiO_2 and Al_2O_3 species via strong covalent link-

ages, (2) one or more hydrophilic quaternary ammonium group that can function as zeolite structure directing agent, and (3) flexible hydrophobic long alkyl tail group, with an adjustable length, which facilitates the creation of mesoscale micelles. In this work, the amphiphilic organosilane (3-(trimethoxysilyl propyl)) hexadecyl dimethyl ammonium chloride (TPHAC) was directly added to the MFI synthesis gel comprising the tetrapropylammonium ion as a structure directing agent for the MFI zeolite. Thereafter, the resulting mixture was hydrothermally treated before being calcined to get rid of the organosilane and the zeolite structure directing agent, leading to the formation of a tailored mesoporous MFI zeolite. The authors declared that the mesopore diameter of the obtained mesoporous MFI zeolite can be finely adjusted, typically in the range of 2–7 nm, based on the length of the organosilane surfactant alkyl chain (C12 to C18) and the synthesis temperature. Likewise, hierarchical mesoporous zeolites with diverse framework topologies, such as MFI, LTA, FAU, MEL, MTW, BEA, AFI, and CHA were successfully prepared.

With the above in mind, in this article, hierarchical mesoporous ZSM-5 zeolites (HM-ZSM-5-x) were synthesized via the soft-template approach, employing organosilane surfactant, 3-[(trimethoxysilyl) propyl]octyldimethyl-ammonium chloride, as a mesopore-forming agent, in the presence of the conventional micropore template, TPAOH. The molecular structure of TPOAC is provided in Figure 1. The impact of the addition amounts of OPAC on the structural and porous properties of the synthesized samples was assessed. Moreover, the catalytic performance was reckoned for the isomerization of *o*-xylene and compared to that of the microporous counterpart. The hierarchical structure and the consequent facile accessibility of active sites inside the ZSM-5 structure endowed the obtained HM-ZSM-5-0.15 catalyst with relatively higher *o*-xylene conversion and *p*-xylene yield compared with the conventional microporous ZSM-5 zeolite.

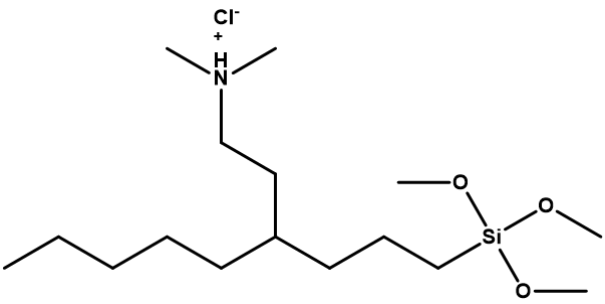

Figure 1. The molecular structure of TPOAC.

2. Materials and Methods

2.1 Chemicals

Tetrapropylammonium hydroxide (TPAOH, 25 wt% in water) was purchased from Acros Organics. Tetraethyl orthosilicate (TEOS, 98 wt%), aluminum isopropoxide (AIP, ≥98 wt%) and 3-[(trimethoxysilyl) propyl]octyldimethyl-ammonium chloride (TPOAC, 42 wt% in methanol), were supplied by Aldrich. All chemicals were used as received without any further purification. Bidistilled water was used in all experiments.

2.2 Catalyst Preparation

Hierarchical mesoporous ZSM-5 zeolites were synthesized via the hydrothermal methodology employing TPOAC as a mesogenous template. In a typical synthesis, initially, certain amounts of AIP and TPAOH were dissolved in bidistilled water in a polypropylene bottle under vigorous stirring at room temperature for about 1 h till complete dissolution. Af-

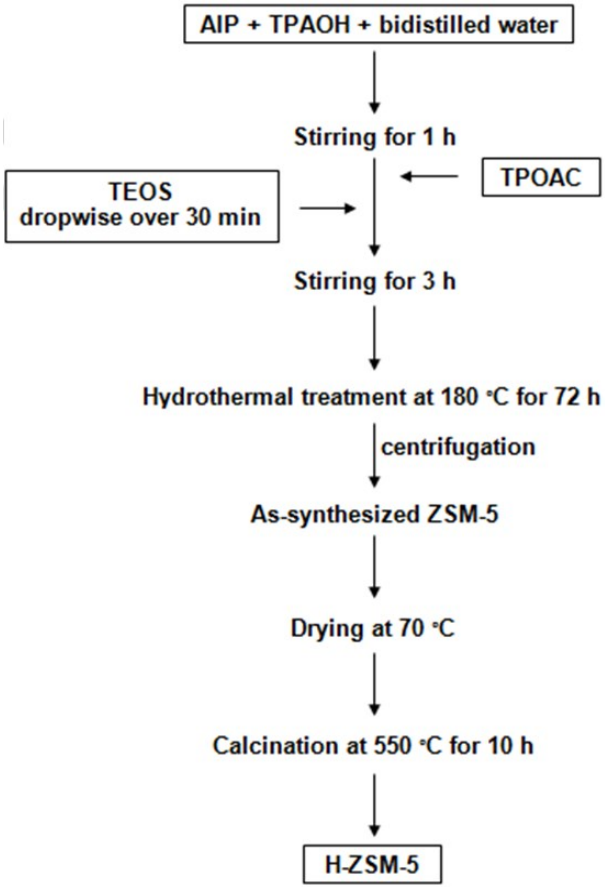

Figure 2. Synthesis process for the preparation of HM-ZSM-5-x zeolites using TPOAC.

ter appropriate amounts of TPOAC were added to the above solution under strong stirring, TEOS was added drop by drop over a period of 30 min. The resulting mixture was allowed to stir for 3 h a room temperature before being transferred into a 100 mL Teflon container inside a stainless-steel autoclave. Then, the autoclave was tightly sealed and heated for 72 h at 180 ºC under autogenous pressure before it was cooled down naturally to room temperature. The resulting white product was isolated from the solution via centrifugation at 10000 rpm/min for 5 min, washed several times with bidistilled water, dried at 70 °C overnight and finally calcined at 550 °C in airflow (100 ml/ min) for 10 h in a tube furnace with a heating rate of 5 °C/min. Figure 2 displays a schematic illustration summarizing the recipe adopted for the preparation of mesoporous ZSM-5 zeolites. For comparison purposes, we also prepared a conventional microporous ZSM-5 sample following a nearly identical synthetic route to that of the hierarchical mesoporous ZSM-5 zeolites except that no TPOAC was added and was named micro-ZSM-5. Additionally, a microporous ZSM-5 molecular sieve, termed micro-ZSM-5, was fabricated as per the reported method of Sabarish and Unnikrishnan [33].

2.2 Catalyst Characterizations

X-ray powder diffraction patterns were obtained with a Brucker AXS-D8 Advance diffractometer using nickel-filtered with Cu-Kαradiation (λ = 1.5405Å) at 30 Kev and 40 mA with a scanning speed of 4° min^{-1} over diffraction angle range. The textural properties of the obtained zeolites were determined from N_2 adsorption-desorption isotherms measured at liquid nitrogen temperature (−196 °C) using a Quantachrome Nova 3200S instrument. HRTEM imaging was conducted on a JEOL JEM-2100F microscope operated at an accelerating voltage of 200 kV. Fourier transform infrared (FT-IR) spectra, in the range of 4000–400 cm^{-1}, were obtained on an ATI Unicam (Mattson 936) Bench Top spectrometer using pressed KBr pellets.

The Brönsted acid sites of the ZSM-5 zeolites were estimated via cationic exchange, adopting NaCl as an exchanging reagent, following the procedure previously described by Serrano *et al*. [34]. Typically, a certain amount of zeolite was placed in 20 g of 1M aqueous NaCl solution and stirred at 60 ºC for 12 h. Afterward, the liberated protons were titrated with 0.01 M aqueous NaOH solution.

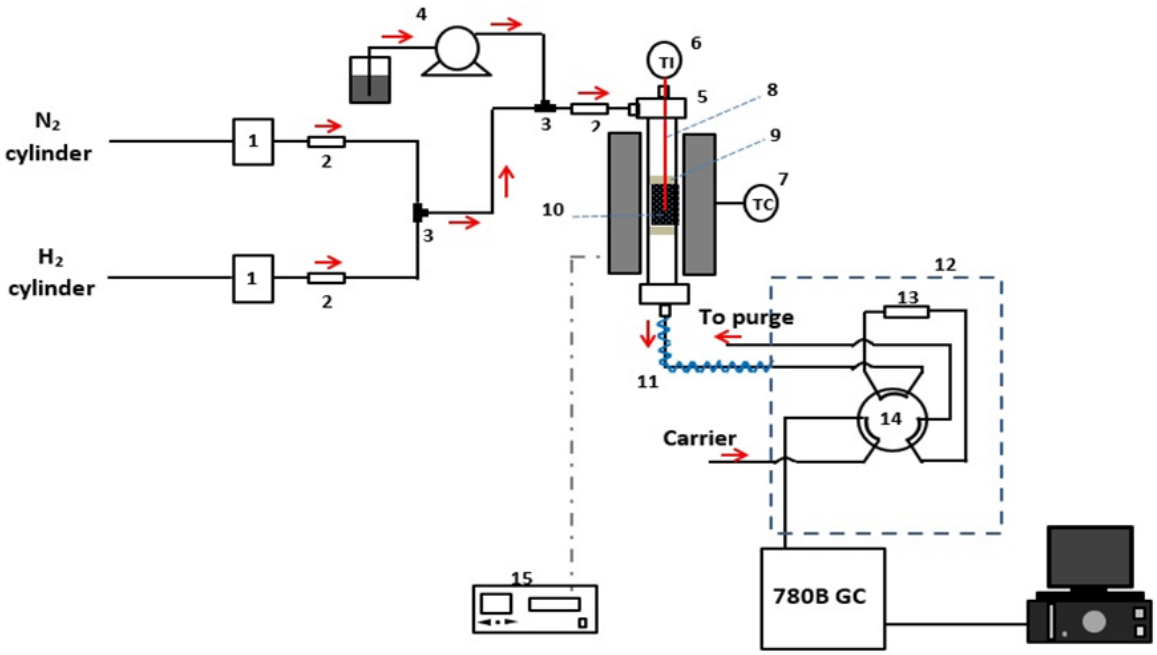

Figure 3. A schematic diagram for the fixed bed flow reactor. 1: Mass flow controller; 2: non-return valve; 3: Tee, 4: pump; 4: three-way valve; 5: stainless steel reactor; 6: temperature indicator; 7: temperature controller; 8: thermocouple; 9: quartz wool; 10: catalyst bed; 11: heating tap; 12: hot box; 13; sample loop; 14: six-port valve; 15: furnace controller (Adapted from [4], Copyright (2022) with permission from Springer Nature).

2.3 Catalytic Tests

The catalytic isomerization of xylene was carried out in a fixed-bed reactor at atmospheric pressure in the temperature range of 250-400 °C. A detailed scheme of this unit is shown in Figure 3. 0.5 g of zeolite catalysts (20-50 mesh) were packed in the center of a stainless-steel reactor (i.d. 1 cm, length 25 cm) and heated by using a tubular furnace. o-Xylene was fed (WHSV = 1 h^{-1}) by a syringe pump. The reaction products were analyzed by an online Agilent 780B GC apparatus equipped with an FID detector and an DB-WAX capillary. The sample inlet temperature was 230 °C and FID temperature was 280 °C. The column temperature was initially kept at 80 °C for 7 min and was then heated to 120 °C with a heating rate of 10 °C/min. Nitrogen was used as carrier gas at a flow-rate of 1 mL/min.

The o-xylene (OX) conversion, p-xylene (PX) yield and p-xylene selectivity were defined as below [35–37]:

$$OX\ conversion\ (\%) = \frac{OX_{feed} - OX_{product}}{OX_{feed}} \times 100 \quad (1)$$

$$PX\ yield\ (\%) = \frac{PX_{product}}{OX_{feed}} \times 100 \quad (2)$$

$$PX\ selectivity\ (\%) = \frac{PX\ yield}{OX\ conversion} \times 100 \quad (3)$$

3. Results and Discussion

3.1 Catalyst Characterizations

In the current investigation, hierarchical mesoporous ZSM-5 zeolites were synthesized using the co-templates of TPAOH and TPOAC by adding different quantities of TPOAC in the conventional ZSM-5 synthetic gel. The X-ray diffraction diffractograms of the as-obtained HM-ZSM-5-x samples are shown in Figure 4. The diffractogram of the microporous counterpart is also presented in the same figure for comparison purposes. All samples displayed diffraction lines at 2θ of 7.86°, 8.78°, 14.78°, 23.18°, 23.90° and 24.40°, which can be readily attributed to ZSM-5 zeolite (JCPDS no. 43-0321), suggesting that all samples have the MFI framework topology [9,38]. No extra diffraction lines related to other zeolitic phases or amorphous silica were detected in the diffract grams, indicating the high phase purity of the synthesized zeolites. Moreover, it is obvious that the intensity of XRD peaks characteristic of ZSM-5 decreases with the increase of TPOAC to SiO_2 molar ratios, suggesting that more organosilane in the synthesis gel results in a decrease in the crystallinity of the obtained hierarchical zeolites. Several previous studies have reported a lowering in the crystallinity of zeolite crystals upon the introduction of a secondary mesopore network [8,11]. The decrease in the crystallization degree would result in an enhancement in the degree of pore connectivity of the synthesized mesoporous zeolite, making the diffusion of the bulk reacting species through the zeolite channels easier, which is beneficial for catalytic applications.

The surface chemistries of the hierarchical mesoporous and microporous ZSM-5 zeolite samples were dissected using the FTIR technique, and the obtained spectrograms are presented in Figure 5. A broad peak can be noticed at the range of 3200-3450 cm^{-1} and was reckoned to arise from the stretching vibration of the siloxane as well as −OH groups [9,39]. The peaks identified at approximately 1225 and 1102 cm^{-1} are most likely a sign of the external and internal asymmetric stretching vibration

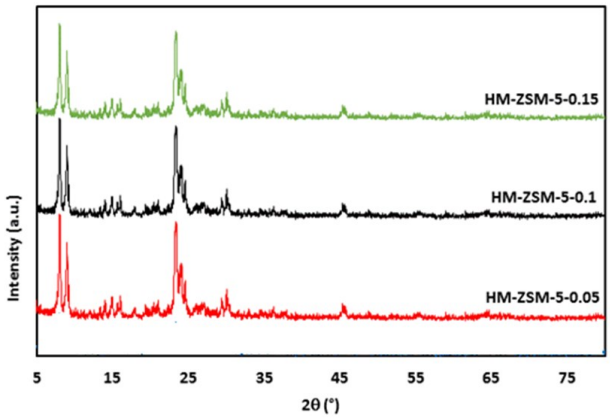

Figure 4. XRD patterns of the micro-ZSM-5 and the hierarchical HM-ZSM-5-x zeolites with different TPOAC to SiO_2 molar ratios.

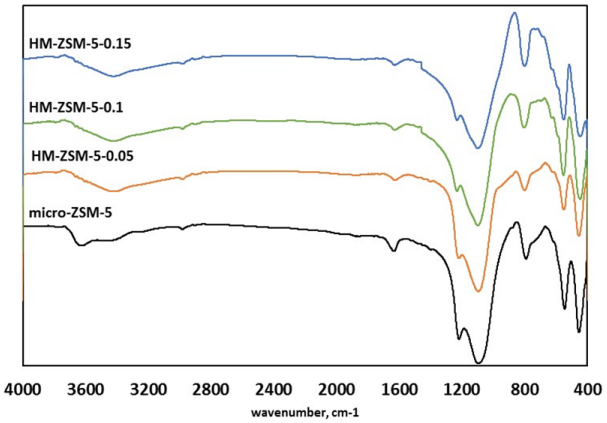

Figure 5. FT-IR spectra of the micro-ZSM-5 and the hierarchical HM-ZSM-5-x zeolites with different TPOAC to SiO_2 molar ratios.

of the Si−O−T in ZSM-5, respectively [39,40], while that perceived at 1644 cm^{-1} denoted physically adsorbed water on the surface of the zeolite [9,38]. Besides, the spectrum revealed a prominent peak at 792 cm^{-1}, which may be designated to the symmetric stretching of the siloxane groups [40,41]. The stretching vibrations five-member ring and the bending vibrations of tetrahedral units of the molecular sieve produced the obvious absorption peaks at around 545 and 447 cm^{-1} [39,41−43]. This further verified that both the micro-and mesoporous zeolites possess the characteristic MFI structure, in line with XRD results.

To entirely understand the porous features of the synthesized zeolites, nitrogen sorption

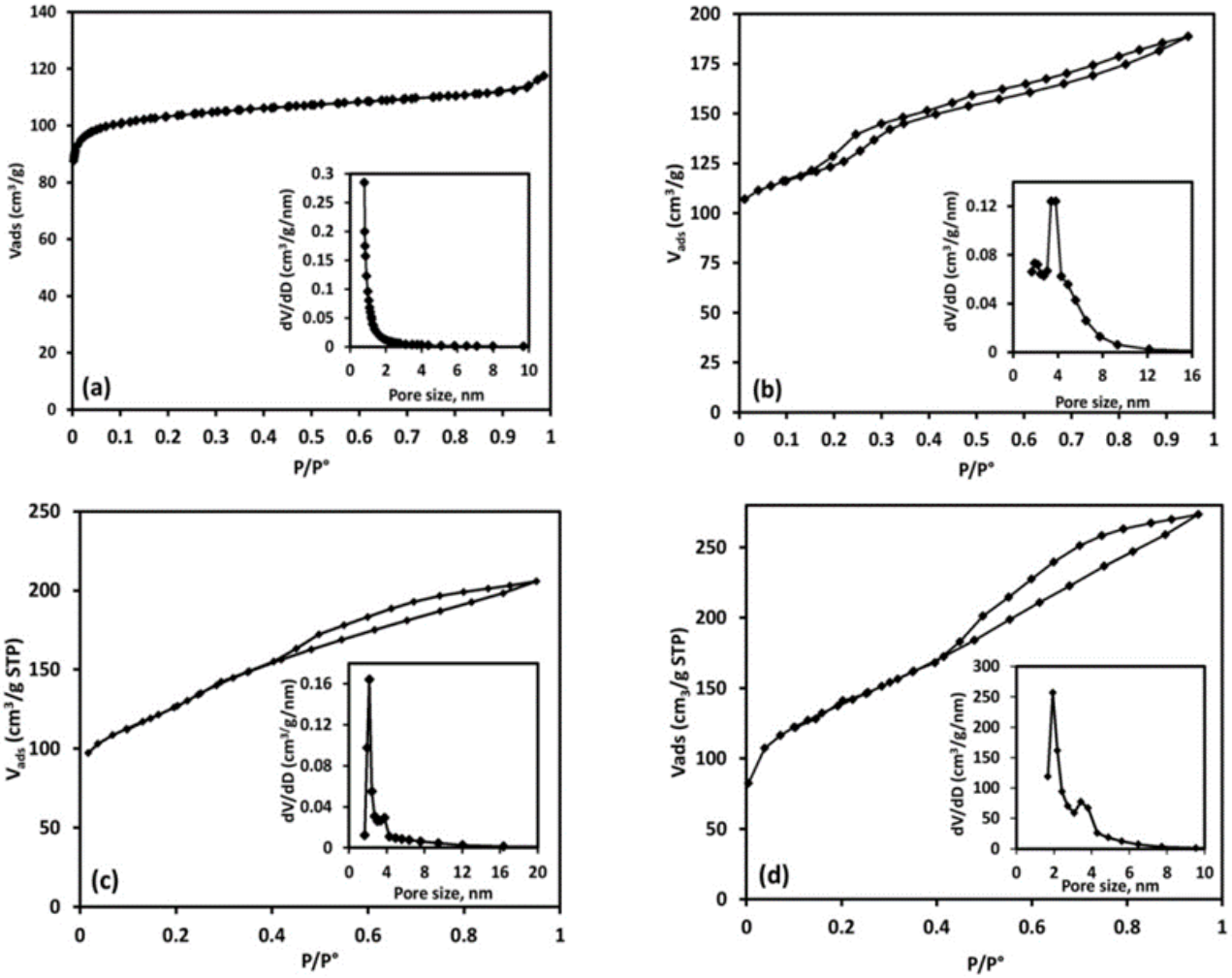

Figure 6. N_2 sorption isotherms and BJH pore size distribution plots (inset) of the micro-ZSM-5 (a), and the hierarchical HM-ZSM-5-x zeolites with different TPOAC to SiO_2 molar ratios (b-d) (a: Reprinted from [9], Copyright (2021) with permission from Elsevier).

Table 1. Textural properties of the micro-ZSM-5 and the hierarchical HZSM-5 zeolites with different with different TPOAC to SiO_2 molar ratios.

Sample	Surface area (m^2/g)			Pore volume (cm^3/g)			Acidity, mmol/g[g]
	S_{BET}[a]	S_{Micro}[b]	S_{Meso}[c]	V_{Total}[d]	V_{Micro}[e]	V_{Meso}[f]	
micro- ZSM-5	311	280	31	0.15	0.135	0.015	0.61
H-ZSM-5-0.05	427	218.5	208.5	0.29	0.106	0.184	n.d.
H-ZSM-5-0.1	472	179.1	292.9	0.32	0.085	0.235	n.d.
H-ZSM-5-0.15	485.64	120.9	364.74	0.422	0.055	0.367	0.41

[a] BET surface area; [b] Micropore surface area evaluated via t-plot method; [c] Mesopore surface area = S_{BET}-S_{Micro}; [d] Total pore volume at P/P^0 = 0.99; [e] Micropore volume evaluated via t-plot method; [f] Mesopore volume = V_{Total}-V_{Micro}; [g] Determined by titration with NaOH solution.

analysis at −196 °C was conducted. The obtained isotherms and the Barrett-Joyner-Halenda (BJH) pore size distribution plots are depicted in Figure 6. Additionally, the textural features of the obtained solids are compiled in Table 1. The isotherm of the micro-ZSM-5 sample belongs to the type I (Figure 6(a)), signifying the microporous characteristic of this sample. According to the BJH pore distribution curve (Figure 6(a)), micro-ZSM-5 is a microporous material with a mean pore diameter of ~1.6 nm with a small number of mesopores, mainly in the 2–4 nm pore size range. Furthermore, as demonstrated in Table 1, the specific surface area and total pore volume of the micro-ZSM-5 were 311 $m^2.g^{-1}$ and 0.155 $cm^3.g^{-1}$, respectively, with a very small contribution of mesoporosity.

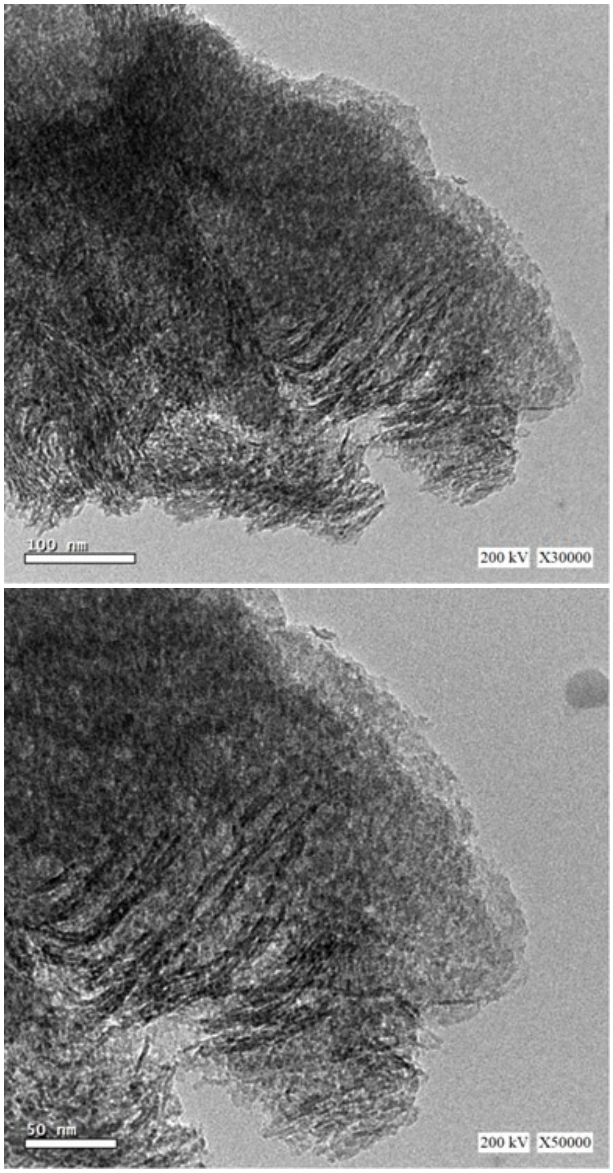

Figure 7. TEM images of HM-ZSM-5-0.15.

As for the HM-ZSM-5-x samples, the resultant N_2 sorption isotherm is clearly different from that of the conventional microporous counterpart. It displayed a mixed type I–IV isotherms, illuminating that the synthesized HM-ZSM-5-x samples have a complex hierarchical porous structure containing micropores and mesopores (Figure 6(b-d)) [44–46]. Indeed, the isotherms unveil two N_2 uptake steps; the first, in the low-pressure range, is fast and is attributed to micropore filling, and latter slower step, which was assigned to the presence of mesopores in the HM-ZSM-5-x materials. Additionally, a distinctive hysteresis loop, which can be seen in the P/Po region from 0.4 to 1.0 bar, represented the filling of the mesopores by capillary condensation. Agreeing with this result, the BJH pore-size distribution plots (Figure 6(b-d)) revealed that HM-ZSM-5-x samples possessed both micro- and mesopores.

As can be seen in Table 1, all HM-ZSM-5-x samples have higher surface areas and pore volumes than the micro-ZSM-5 sample. Such improvement in the surface area and pore volume could presumably be ascribed to the presence of mesopores in HM-ZSM-5-x samples. It's worth mentioning that, in contrast to the micro-ZSM-5 sample in which the mesoporous surface area and pore volume constitute only a small portion of the total surface area and pore volume, the vast majority of the total surface area and pore volume of HM-ZSM-5-x was emanated from the mesopores. The dominant mesoporous character of the HM-ZSM-5-x allows the fast diffusion of bulky adsorbate molecules through its interior porous system to access the active binding sites and consequently would be beneficial for catalytic applications, especially those involving large substrates [47]. The hierarchical samples displayed much larg-

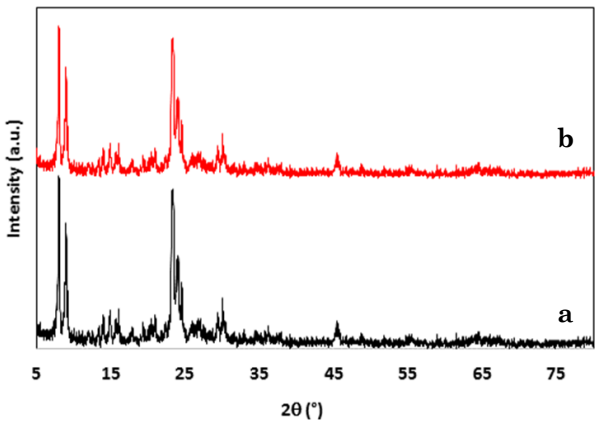

Figure 8. XRD of H-ZSM-5-0.15 sample before (a) and after (b) submersion in boiling water for 5 days.

er mesoporous surface area and pore volume as compared to the conventional micro-ZSM-5. As observed in Table 1, the increase in the amounts of the mesopore-gene (TPOAC) led to a remarkable increase in the surface areas, mesopore volumes, and mesopore areas of HM-ZSM-5-x samples, demonstrating that the mesoporosity of the obtained HM-ZSM-5-x zeolites can be simply tuned through the variation of the amount of TPOAC used. On the contrary, the micropore volumes and micropore areas of HM-ZSM-5-x samples are less than that of the conventional ZSM-5 sample and were found to decrease gradually with the increase of the amount of TPOAC.

Figure 7 exhibits the TEM images of HM-ZSM-5-0.15. HM-ZSM-5-0.15 was selected since it has the largest mesoporosity among the hierarchical zeolite samples, as demonstrated by N_2 sorption measurements. The TEM images revealed the creation of a 3d mesoporous network within the mesoporous zeolite crystal. This continuous mesoporous network would allow for the easy diffusion of the reactants and products through the network during the catalytic process and hence is expected to boost the isomerization performance of the catalyst [48].

Moreover, to check the hydrothermal stability of the synthesized hierarchical zeolites, the HM-ZSM-5-0.15 sample, after submersion in boiling water for 5 days, was characterized by XRD. The XRD patterns of the HM-ZSM-5-0.15 sample before and after soaking in boiling water are shown in Figure 8. Inspection of this figure revealed that the XRD pattern of the HM-ZSM-5-0.15 after soaking was essentially identical to that of the pristine one, confirming that HM-ZSM-5-0.15 was hydrothermally stable.

The thermal behavior of micro-ZSM-5 and HM-ZSM-0.15 samples was assessed by the thermal gravimetric analysis (TGA), and the

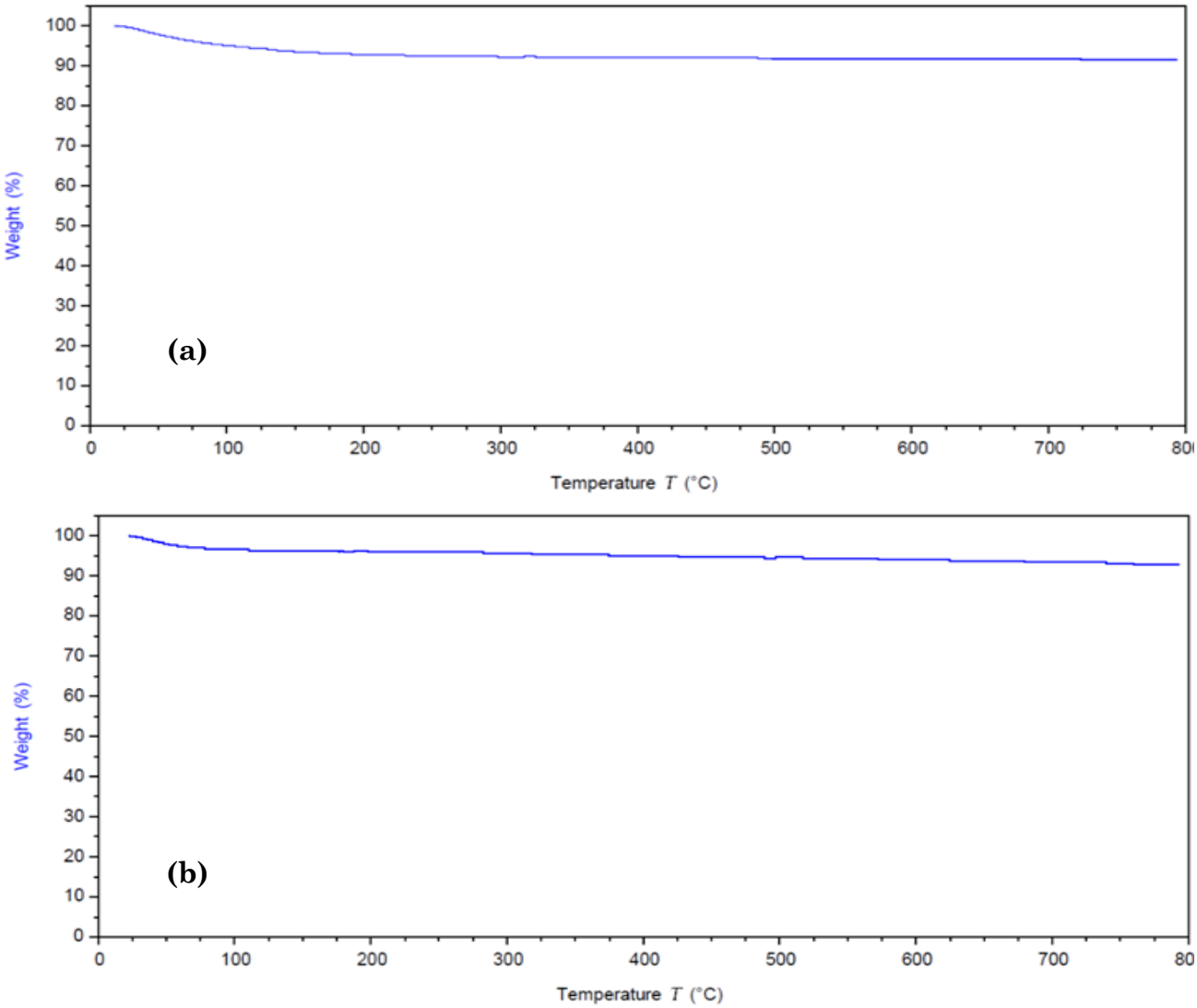

Figure 9. TGA curves of the micro-ZSM-5 (a), and the H-ZSM-5-0.15 sample (b).

resultant TGA thermograms are shown in Figure 9. As seen in Figure 9, the TGA thermograms for the two samples manifested only one thermal event of weight loss in the range of 25 to 150 °C, related to the thermodesorption of physically adsorbed water. For both samples, there were no other thermal events at temperatures exceeding 150 °C. Based on these results, it can be deduced that both the micro-ZSM-5 and the hierarchical molecular sieves have almost the same thermal stabilities and seem to be thermally stable in the temperature range where the isomerization reaction is performed.

3.2 o-Xylene Isomerization

The catalytic properties of the HM-ZSM-5-0.15 sample were evaluated in the isomerization of o-xylene to p-xylene. All isomerization experiments were conducted in a continuous-flow reactor under the following conditions: temperatures of 250-400 °C, pressure of 1 bar, and a space velocity of 1 h^{-1}. The isomerization reaction was also conducted using the conventional micro-ZSM-5 catalyst under the same experimental conditions in order to clarify the role of the mesoporosity in the HM-ZSM-5-0.15 catalyst in the isomerization of o-xylene. The main reaction products of the o-xylene conversion were: the other two xylene isomers (isomerization products), along with low amounts of the trimethylbenzenes and toluene (disproportionation products), regardless of the catalyst used. Figure 10(A) presents the profile of o-xylene isomerization with reaction temperature using the same amount of zeolite catalyst. Results unveiled that catalyst mesoporosity had a profound effect on the catalytic activity. Under the applied conditions, the micro-ZSM-5 sample manifested lower activity at all reaction temperatures. For example, at 400 ºC, for HM-ZSM-5-0.15 zeolite, the initial o-xylene conversion was 57.0%, while the initial conversion for micro-ZSM-5 was only nearly 39.2%. Based on the titration results in Table 1, the acidity of the hierarchical mesoporous zeolite was lower than that of the conventional microporous zeolite, indicating that catalyst acidity was not the main parameter governing the isomerization process. So, the low activity of the micro-ZSM-5 sample was mainly due to the sole presence of micropores that imposed diffusion limitation, leading to low utilization of the catalyst active centers and fast coke deposition. In other words, the higher catalytic activity of the HM-ZSM-5-0.15 catalyst than the micro-ZSM-5 catalyst can be ascribed to the decrease of diffusion limitation such that o-xylene molecules can readily access the acidic active centers within the zeolite catalysts [49]. On the contrary, the initial p-xylene selectivity over hierarchical ZSM-5 zeolite was very slightly lower than that of the micro-ZSM-5 zeolite, indicating that the introduced mesoporosity had

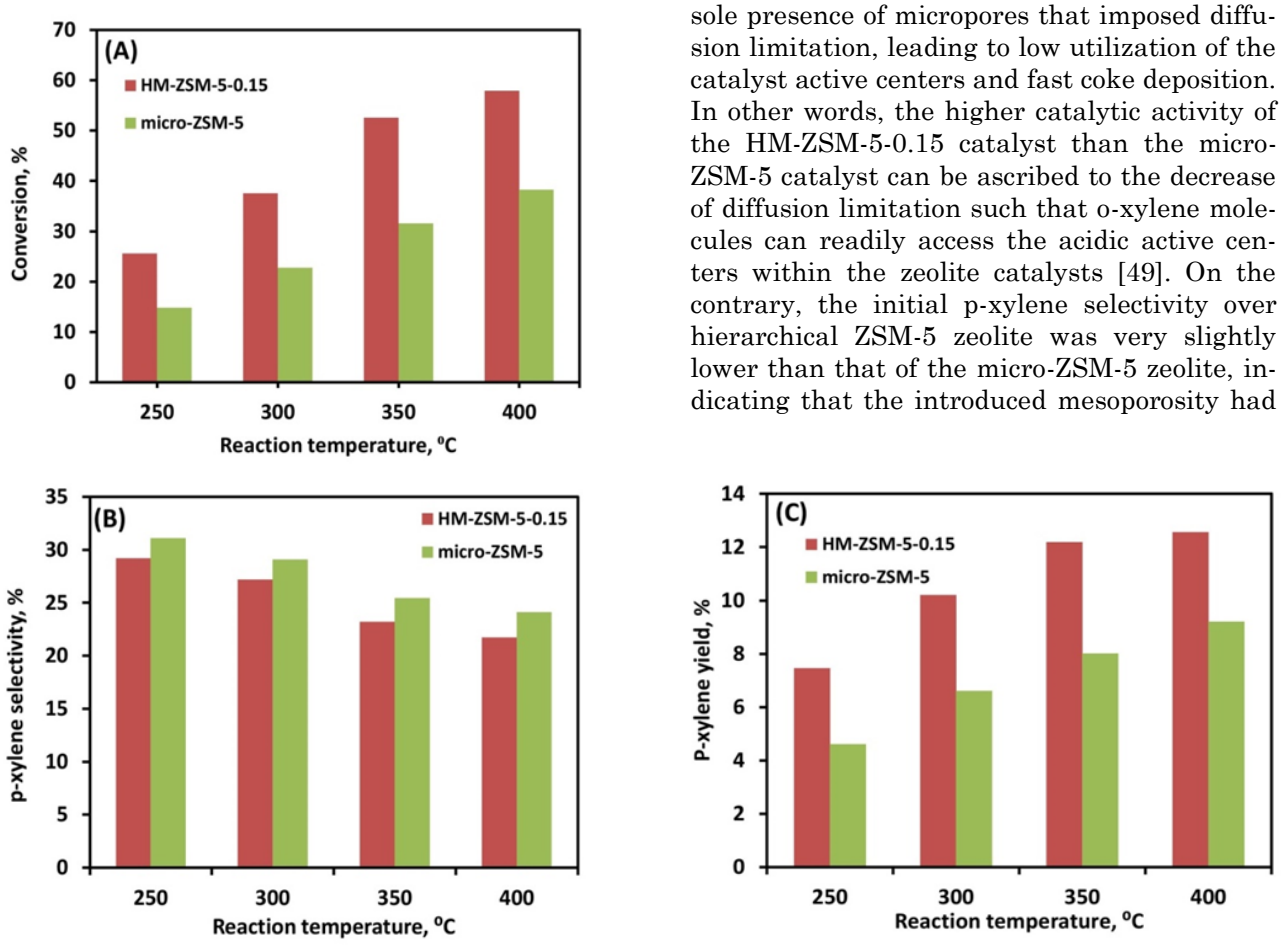

Figure 10. The effect of reaction temperature on xylene conversion (A), p-xylene yield (B), and p-xylene selectivity (C).

a slight negative effect on p-xylene selectivity, Figure 10(B) [49,50]. Therefore, HM-ZSM-5-0.15 gave a higher p-xylene yield than the micro-ZSM-5. Figure 10(C). Zhou *et al.* [48] successfully prepared hierarchical mesoporous ZSM-5 zeolite via steam-assisted crystallization. The catalyst was utilized for the isomerization of o-xylene. The catalyst achieved an o-xylene conversion of 51.6%, p-xylene yield of 11.6%, and p-Xylene selectivity of 22.4% when the reaction was conducted at a temperature of 500 °C with a catalyst mass of 0.1 g and nitrogen flow of 50 mL.min^{-1}.

Importantly, the catalyst manifested superb operational stability within 50 h (Figure 11). The o-xylene conversion was decreased from an initial value of 57.9% to 48.61% after the time of stream of 50 h. Meanwhile, the p-xylene yield remained virtually constant at 12.61%. The excellent stability of the catalyst can be ascribed to the presence of mesopores in its structure, which endowed the catalyst with high resistance against deactivation through coke deposition.

4. Conclusions

In conclusion, hierarchical micro-mesoporous structured ZSM-5 zeolite catalysts (HM-ZSM-5-x) for o-Xylene isomerization were introduced. These catalysts were prepared via the hydrothermal route in the combined presence of TPAOH and the organosilane surfactant, 3-[(trimethoxysilyl) propyl]octyldimethyl-ammonium chloride, as micropore, and mesopore structure-directing agents, respectively. Compared with the classical microporous ZSM-5, these molecular sieves manifested higher surface areas, and pore volumes, with the major portion of this porosity being attributed to mesopores. Accordingly, the molecular sieve with the largest mesoporosity, HM-ZSM-5-0.15, manifested higher o-xylene conversion than the microporous counterpart, which can be ascribed to the reduced diffusion limitation and the augmented active site accessibility. Moreover, the catalyst manifested remarkable operational stability within 50 h, suggesting good tolerance to deactivation by coke formation due to its abundant mesoporous structure. In summary, the fabricated hierarchical micro-mesoporous structured ZSM-5 zeolite catalysts are a promising catalyst for o-xylene isomerization, and are expected to have acceptable performance in diverse chemical reactions, especially those involving large substrates.

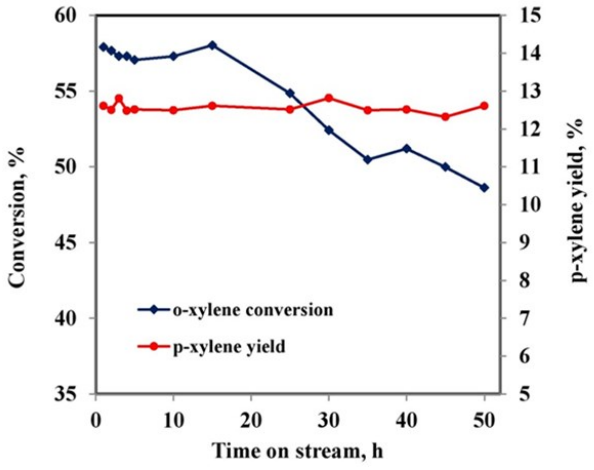

Figure 11. Effect of time on stream on o-xylene conversion, and p-xylene yield over HM-ZSM-5-0.15.

Acknowledgments

This paper is part of the work supported by the Science, Technology & Innovation Funding Authority (STDF), Egypt, Under Grant No.: 10757.

CRediT Author Statement

Ahmed El Fadaly: Methodology, Investigation, Formal Analysis; M.A. Sayed: Methodology, Supervision, Validation; Ahmed O. Abo El Naga: Conceptualization, Methodology, Project Administration, Funding acquisition, Writing–Original Draft; Mohamed El Saied: Supervision, Investigation; Seham A. Shaban: Conceptualization, Supervision, Project Administration, Funding acquisition, Writing–Review and Editing; F.I. Elhosiny: Supervision, Writing–Review and Editing. All authors have read and agreed to the published version of the manuscript.

References

[1] Zhang, B., Xiu, G., Chen, J., Yang, S. (2015). Detonation and deflagration characteristics of p-Xylene/gaseous hydrocarbon fuels/air mixtures. *Fuel*, 140, 73-80. DOI: 10.1016/j.fuel.2014.09.105.

[2] Zepeda, T.A., Pawelec, B., Infantes-Molina, A., Yocupicio, R.I., Alonso-Núñez, G., Fuentes, S., de León, J.N.D., Fierro, J.L.G. (2015). Ortho-xylene hydroisomerization under pressure on HMS-Ti mesoporous silica decorated with Ga2O3 nanoparticles. *Fuel*, 158, 405-415. DOI: 10.1016/j.fuel.2015.05.056.

[3] Nassimbeni, L.R., Báthori, N.B., Patel, L.D., Su, H., Weber, E. (2015). Separation of xylenes by enclathration. *Chemical Communications,* 51, 3627. DOI: 10.1039/C4CC05329J.

[4] Al-Khattaf, S., Tukur, N.M., Al-Amer, A. (2007). 1,2,4Trimethylbenzene Transformation Reaction Compared with its Transalkylation Reaction with Toluene over USY Zeolite Catalyst. *Industrial & Engineering Chemistry Research*, 46, 4459. DOI: 10.1021/ie0702781.

[5] Al-Khattaf, S., Odedairo, T., Balasamy, R.J. (2013). Kinetic and catalytic performance of a BI-porous composite material in catalytic cracking and isomerisation reactions. *The Canadian Journal of Chemical Engineering,* 91, 607. DOI: 10.1002/cjce.21635.

[6] Balasamy, R.J., Odedairo, T., Al-Khattaf, S. (2011). Unique catalytic performance of mesoporous molecular sieves containing zeolite units in transformation of m-xylene. *Applied Catalysis A: General*, 409, 223-233. DOI: 10.1016/j.apcata.2011.10.007.

[7] Wu, Q., Wang, X., Meng, X., Yang, C., Liu, Y., Jin, Y., Yang, Q., Xiao, F.S. (2014). Organotemplate-free, seed-directed, and rapid synthesis of Al-rich zeolite MTT with improved catalytic performance in isomerization of m-xylene. *Microporous and Mesoporous Materials,* 186, 106-112. DOI: 10.1016/j.micromeso.2013.11.043.

[8] Liu, S., Yang, S., He, J., Mao, D., Yin, C. (2021). Efficient synthesis of chain-like ZSM-5 zeolite for the m-xylene isomerization reaction. *Inorganic Chemistry Communications*, 128, 108564. DOI: 10.1016/j.inoche.2021.108564.

[9] Marzouk, N.M., El Naga, A.O.A., Younis, S.A., Shaban, S.A., El Torgoman, A.M., El Kady, F.Y. (2021). Process optimization of biodiesel production via esterification of oleic acid using sulfonated hierarchical mesoporous ZSM-5 as an efficient heterogeneous catalyst. *Journal of Environmental Chemical Engineering*, 9(2), 105035. DOI: 10.1016/j.jece.2021.105035.

[10] da Silva, J.F., da Silva Ferracine, E.D., Cardoso, D. (2022). Improved accessibility of Na-LTA zeolite catalytic sites for the Knoevenagel condensation reaction. *Microporous and Mesoporous Materials,* 331, 111640. DOI: 10.1016/j.micromeso.2021.111640.

[11] Verboekend, D., Nuttens, N., Locus, R., Van Aelst, J., Verolme, P., Groen, J.C., Pérez-Ramírez, J., Sels, B.F. (2016). Synthesis, characterisation, and catalytic evaluation of hierarchical faujasite zeolites: milestones, challenges, and future directions. *Chemical Society Reviews*, 45(12), 3331-3352. DOI: 10.1039/C5CS00520E.

[12] Zhao, C., Hu, X., Liu, C., Chen, D., Yun, J., Jiang, X., Wei, N., Li, M., Chen, Z. (2022). Hierarchical architectures of ZSM-5 with controllable mesoporous and their particular adsorption/desorption performance for VOCs. *Journal of Environmental Chemical Engineering*, 10(1), 106868. DOI: 10.1016/j.jece.2021.106868.

[13] Wang, Q., Xu, S., Chen, J., Wei, Y., Li, J., Fan, D., Yu, Z., Qi, Y., He, Y., Xu, S., Yuan, C., Zhou, Y., Wang, J., Zhang, M., Su, B., Liu, Z. (2014). Synthesis of mesoporous ZSM-5 catalysts using different mesogenous templates and their application in methanol conversion for enhanced catalyst lifespan. *RSC Advances*, 4(41), 21479-21491. DOI: 10.1039/C4RA02695K.

[14] Wei, Y., Parmentier, T.E., de Jong, K.P., Zečević, J. (2015). Tailoring and visualizing the pore architecture of hierarchical zeolites. *Chemical Society Reviews*, 44, 7234-7261. DOI: 10.1039/C5CS00155B.

[15] Möller, M., Bein, T. (2013). Mesoporosity – a new dimension for zeolites. *Chemical Society Reviews*, 42, 3689-3707. DOI: 10.1039/C3CS35488A.

[16] Yutthalekha, T., Wattanakit, C., Warakulwit, C., Wannapakdee, W., Rodponthukwaji, K., Witoon, T., Limtrakul, J. (2017). Hierarchical FAU-type zeolite nanosheets as green and sustainable catalysts for benzylation of toluene. *Journal of Cleaner Production*, 142, 1244-1251. DOI: 10.1016/j.jclepro.2016.08.001.

[17] Arumugam, M., Wong, K.L., Nadarajan, A., Lai, S.Y., Goh, C.K., Triwahyono, S., Taufiq-Yap, Y.H. (2022). Green solvothermal synthesis and characterisation of surface organosilylated hierarchical nanozeolite ZSM-5. *Microporous and Mesoporous Materials*, 329, 111516. DOI: 10.1016/j.micromeso.2021.111516.

[18] Khan, W., Jia, X., Wu, Z., Choi, J., Yip, A.C. (2019). Incorporating hierarchy into conventional zeolites for catalytic biomass conversions: A review. *Catalysts*, 9(2), 127. DOI: 10.3390/catal9020127.

[19] Fernandez, C., Stan, I., Gilson, J.P., Thomas, K., Vicente, A., Bonilla, A., Ramírez, J.P. (2010). Hierarchical ZSM-5 Zeolites in Shape-Selective Xylene Isomerization: Role of Mesoporosity and Acid Site Speciation. *Chemistry – A European Journal,* 16, 6224. DOI: 10.1002/chem.200903426.

[20] Chal, R., Gérardin, C., Bulut, M., van Donk, S. (2011). Overview and industrial assessment of synthesis strategies towards zeolites with mesopores. *ChemCatChem*, 3(1), 67-81. DOI: 10.1002/cctc.201000158

[21] Shanbhag, G.V., Choi, M., Kim, J., Ryoo, R. (2009). Mesoporous sodalite: A novel, stable solid catalyst for base-catalyzed organic transformations. *Journal of Catalysis*, 264(1), 88-92. DOI: 10.1016/j.jcat.2009.03.014.

[22] Inayat, A., Knoke, I., Spiecker, E., Schwieger, W. (2012). Assemblies of mesoporous FAU-type zeolite nanosheets. *Angewandte Chemie*, 51(8), 1962-1965. DOI: 10.1002/anie.201105738.

[23] Meng, X., Nawaz, F., Xiao, F. (2009). Templating route for synthesizing mesoporous zeolites with improved catalytic properties, *Nano Today*, 4, 292. DOI: 10.1016/j.nantod.2009.06.002.

[24] Zhou, J., Hua, Z.L., Liu, Z.C., Wu, W., Zhu, Y., Shi, J.L. (2011). Hollow Mesoporous Zeolite Microspheres: Hierarchical Macro-/meso-/microporous Structure and Exceptionally Enhanced Adsorption Properties. *Dalton Transactions*, 40, 12667-12669. DOI: 10.1039/C1DT11684C.

[25] Zhu, Y., Hua, Z.L., Zhou, J., Wang, L., Zhao, J., Gong, Y., Wu, W., Ruan, M., Shi, J.L. (2011). Hierarchical Mesoporous Zeolites: Direct Self-Assembly Synthesis in a Conventional Surfactant Solution by Kinetic Control over the Zeolite Seed Formation. *Chemistry – A European Journal,* 17, 14618–14627. DOI: 10.1002/chem.201101401.

[26] Serrano, D.P., García, R.A., Vicente, G., Linares, M., Procházková, D., Čejka, J. (2011). Acidic and catalytic properties of hierarchical zeolites and hybrid ordered mesoporous materials assembled from MFI protozeolitic units. *Journal of Catalysis*, 279, 366–380. DOI: 10.1016/j.jcat.2011.02.007.

[27] Song, J., Ren, L., Yin, C., Ji, Y., Wu, Z., Li, J., Xiao, F.S. (2008). Stable, Porous, and bulky Particles with High External Surface and Large Pore Volume from Self-assembly of Zeolite Nanocrystals with Cationic Polymer. *The Journal of Physical Chemistry C*, 112, 8609–8613. DOI: 10.1021/jp800598p.

[28] Wang, H., Pinnavaia, T.J. (2006) MFI Zeolite with Small and Uniform Intracrystal Mesopores. *Angewandte Chemie,* 45, 7603–7606. DOI: 10.1002/anie.200602595.

[29] Shetti, V.N., Kim, J., Srivastava, R., Choi, M., Ryoo, R. (2008). Assessment of the mesopore wall catalytic activities of MFI zeolite with mesoporous/microporous hierarchical structures. *Journal of Catalysis*, 254, 296–303. DOI: 10.1016/j.jcat.2008.01.006.

[30] Choi, M., Choi, H.S., Srivastava, R., Venkatesan, C., Choi, D.H., Ryoo, R. (2006). Amphiphilic organosilane-directed synthesis of crystalline zeolite with tunable mesoporosity. *Nature Materials*, 5, 718–723. DOI: 10.1038/nmat1705.

[31] Jacobsen, C.J., Madsen, C., Houzvicka, J., Schmidt, I., Carlsson, A. (2000). Mesoporous Zeolite Single Crystals. *Journal of the American Chemical Society*, 122, 7116. DOI: 10.1021/ja000744c.

[32] Na, K., Choi, M., Ryoo, R. (2013). Recent advances in the synthesis of hierarchically nanoporous zeolites. *Microporous and Mesoporous Materials*, 166, 3-19. DOI: 10.1016/j.micromeso.2012.03.054.

[33] Sabarish, R., Unnikrishnan, G. (2020). A novel anionic surfactant as template for the development of hierarchical ZSM-5 zeolite and its catalytic performance. *Journal of Porous Materials,* 27, 691-700. DOI: 10.1007/s10934-019-00852-5.

[34] Serrano, D.P., Pinnavaia, T.J., Aguado, J., Escola, J.M., Peral, A., Villalba, L. (2014). Hierarchical ZSM-5 zeolites synthesized by silanization of protozeolitic units: Mediating the mesoporosity contribution by changing the organosilane type. *Catalysis Today*, 227, 15-25. DOI: 10.1016/j.cattod.2013.10.052.

[35] Yeong, Y.F., Abdullah, A.Z., Ahmad, A.L., Bhatia, S. (2010). Synthesis, characterization and reactive separation activity of acid-functionalized silicalite-1 catalytic membrane in m-xylene isomerization. *Journal of Membrane Science*, 360(1-2), 109-122. DOI: 10.1016/j.memsci.2010.05.009.

[36] Farshadi, M., Falamaki, C. (2018). Ethylbenzene disproportionation and p-xylene selectivity enhancement in xylene isomerization using high crystallinity desilicated H-ZSM-5. *Chinese Journal of Chemical Engineering*, 26(1), 116-126. DOI: 10.1016/j.cjche.2017.03.023.

[37] Rasouli, M., Atashi, H., Mohebbi-Kalhori, D., Yaghobi, N. (2017). Bifunctional Pt/Fe-ZSM-5 catalyst for xylene isomerization. *Journal of the Taiwan Institute of Chemical Engineers*, 78, 438-446. DOI: 10.1016/j.jtice.2017.05.018.

[38] He, L.C., Xu, H.H., Leng, X.Y., Jin, L.Y., Jia, A.P., Luo, M.F., Chen, J. (2023). Boosting diethylamine selective oxidation over CuO/ZSM-5 catalyst by CeO_2 modification. *Fuel*, 342, 127792. DOI: 10.1016/j.fuel.2023.127792.

[39] Sadeghi, M., Farhadi, S., Zabardasti, A. (2020). Magnetic separable zeolite-type ZSM-5/CdS nanorods/MoS_2 nanoflowers/$MnFe_2O_4$ quaternary nanocomposites: synthesis and application of sonocatalytic activities. *New Journal of Chemistry*, 44(47), 20878-20894. DOI: 10.1039/D0NJ04056H.

[40] Cui, Y., Chen, B., Xu, L., Chen, M., Wu, C. E., Qiu, J., Cheng, G., Wang, N., Xu, J., Hu, X. (2023). CO_2 methanation over the Ni-based catalysts supported on the hollow ZSM-5 zeolites: Effects of the hollow structure and alkaline treatment. *Fuel*, 334, 126783. DOI: 10.1016/j.fuel.2022.126783.

[41] Subagyo, R., Tehubijuluw, H., Utomo, W.P., Rizqi, H.D., Kusumawati, Y., Bahruji, H., Prasetyoko, D. (2022). Converting red mud wastes into mesoporous ZSM-5 decorated with TiO_2 as an eco-friendly and efficient adsorbent-photocatalyst for dyes removal. *Arabian Journal of Chemistry,* 15(5), 103754. DOI: 10.1016/j.arabjc.2022.103754.

[42] Maharani, D.K., Kusumawati, Y., Safitri, W. N., Nugraha, R.E., Holilah, H., Sholeha, N.A., Jalilm, A.A., Bahruji, H., Prasetyoko, D. (2023). Optimization of hierarchical ZSM-5 structure from kaolin as catalysts for biofuel production. *RSC Advances*, 13(21), 14236-14248. DOI: 10.1039/D3RA01810E.

[43] Cui, Y., Qiu, J., Chen, B., Xu, L., Chen, M., Wu, C.E., Cheng, G., Yang, B., Wang, N., Hu, X. (2022). CO_2 methanation over Ni/ZSM-5 catalysts: The effects of support morphology and La_2O_3 modification. *Fuel*, 324, 124679. DOI: 10.1016/j.fuel.2022.124679.

[44] Youssef, N.A.E., Amer, E., El Naga, A.O.A., & Shaban, S.A. (2020). Molten salt synthesis of hierarchically porous carbon for the efficient adsorptive removal of sodium diclofenac from aqueous effluents. *Journal of the Taiwan Institute of Chemical Engineers*, 113, 114-125. DOI: 10.1016/j.jtice.2020.07.018.

[45] Hussein, M.F., El Naga, A.O.A., El Saied, M., AbuBaker, M.M., Shaban, S.A., El Kady, F.Y. (2021). Potato peel waste-derived carbon-based solid acid for the esterification of oleic acid to biodiesel. *Environmental Technology & Innovation*, 21, 101355. DOI: 10.1016/j.eti.2021.101355.

[46] Dahshan, A., Saddeek, Y.B., Aly, K.A., Shaaban, K.H.S., Hussein, M.F., El Naga, A.O.A., Shaban, S.A., Mahmoud, S.O. (2019). Preparation and characterization of $Li_2B_4O_7$–TiO_2–SiO_2 glasses doped with metal-organic framework derived nano-porous Cr_2O_3. *Journal of Non-Crystalline Solids*, 508, 51-61. DOI: 10.1016/j.jnoncrysol.2019.01.002.

[47] Mostafa, M.S., El Naga, A.O.A., Galhoum, A.A., Guibal, E., Morshedy, A.S. (2019). A new route for the synthesis of self-acidified and granulated mesoporous alumina catalyst with superior Lewis acidity and its application in cumene conversion. *Journal of Materials Science*, 54, 5424-5444. DOI: 10.1007/s10853-018-03270-1.

[48] Zhao, J., Zhou, J., Chen, Y., He, Q., Ruan, M., Guo, L., Shi, J., Chen, H. (2009). Fabrication of mesoporous zeolite microspheres by a one-pot dual-functional templating approach. *Journal of Materials Chemistry*, 19(41), 7614-7616. DOI: 10.1039/B916862A.

[49] Zhou, J., Liu, Z., Li, L., Wang, Y., Gao, H., Yang, W., Xie, Z., Tang, Y. (2013). Hierarchical mesoporous ZSM-5 zeolite with increased external surface acid sites and high catalytic performance in o-xylene isomerization. *Chinese Journal of Catalysis*, 34(7), 1429-1433. DOI: 10.1016/S1872-2067(12)60602-0.

[50] Zhao, Y., Wang, L., Ye, Z., Zhang, H., Xie, S., Zhang, Y., Tang, Y. (2019). Constructing mosaic-tiling MFI zeolite mesocrystal with enhanced catalytic performance. *Crystal Growth & Design*, 19(11), 6192-6198. DOI: 10.1021/acs.cgd.9b00625.